

Epoxy thiol photolatent base clearcoats: curing and formulation

Christopher M. Seubert, Mark E. Nichols

© FSCT and OCCA 2010

Abstract Photolatent base crosslinked epoxy thiol coatings were characterized using transmission FTIR spectroscopy, Raman spectroscopy, UV spectroscopy, and Vickers micro-hardness testing. Curing rate constants were calculated for a series of formulations with varying concentrations of photolatent-DBN, ITX (2-isopropyl thioxanthone), and BP (benzophenone), as well as varying curing times. A design of experiments demonstrated that increased UV dose had the greatest impact on increasing the curing rate of the clearcoat system. BP wt% proved to have little impact on the clearcoat curing rate, while PL-DBN and ITX exhibited minimal improvement above 2.5 wt% and 1 wt%, respectively. Vickers micro-hardness results showed that irradiation dose had no impact on the final physical properties of the clearcoat. However, a 24-h ambient post-cure proved to increase the final hardness of the clearcoat under some conditions.

Keywords UV cure, Clearcoat, Photolatent base, Epoxy, Thiol, Kinetics

Introduction

Automotive clearcoats were introduced in the mid-1980s to improve the appearance and long-term performance of automotive paint systems. Since then, these coatings have evolved into very robust systems with excellent durability. The chemistry on which OEM clearcoats are based includes, but is not limited to, acrylic-melamine, urethane, acrylic-silane-melamine, epoxy acid, and carbamate. These thermoset coatings require the addition of significant amounts of organic solvents to achieve spray viscosities and also require a

thermal curing step of ~130°C for 20–30 min to achieve acceptable physical properties.

While the previously mentioned clearcoat chemistries broadly satisfy the requirements for an acceptable clearcoat, significant improvements could be made in the areas of scratch resistance, energy required to crosslink the coatings, and VOC levels. One possible solution is the use of UV curable clearcoats.^{1,2} UV curable clearcoats have long been used in nonautomotive industries due to their unique advantages. When exposed to UV light, the photoinitiator additives in the clearcoat cleave to form free radicals, which initiates crosslinking. These coatings have the potential to cure very quickly (seconds), achieve high scratch resistance (high crosslink densities), achieve zero VOC formulations, and eliminate the need to thermally cure the coating.^{3,4} Current free radical UV curable clearcoats require direct UV light exposure in order to fully crosslink the coating. This is very difficult to accomplish if the coating is applied to a complex, three-dimensional shape, such as an automobile. Dual cure coatings were introduced as one potential solution to this problem.³ These coatings contain both UV and thermal curing components such that shadowed regions will become partially cured when heated. Unfortunately, this still requires the use of an oven, thereby limiting any energy and time benefits associated with the removal of a curing oven.

Unique UV curable clearcoat chemistries have been developed that not only have the ability to cure upon exposure to UV light, but that also will slowly cure, even with little or no UV exposure. Cationically cured clearcoats are one such type of clearcoat.⁵ These clearcoats have photoinitiators that decompose into strong acid catalysts upon exposure to UV radiation.^{3,6} The acid catalyst initiates the crosslinking reaction to facilitate the curing of the clearcoat. Coatings cured by photolatent base photoinitiators have recently been reported.⁷ These coating chemistries cure when

C. M. Seubert (✉), M. E. Nichols
Ford Motor Company, Dearborn, MI, USA
e-mail: cseubert@ford.com

exposed to a base catalyst, which in this case is introduced when photoinitiator is exposed to UV light and dissociates to form 1,5-diazabicyclo[4.3.0]-non-5-ene (DBN), a strong base catalyst (Fig. 1). Similar to cationically cured coatings, these systems do not exhibit oxygen inhibition due to their curing mechanism.

A number of photolatent base clearcoat chemistries are being explored in the laboratory as well as in practice.^{7,8} A commercial thio-urethane clearcoat system has recently been developed for the automotive refinish industry.⁹ The system cures upon exposure to UV-A light, but not as quickly as traditional free radical cure clearcoats. Other base-catalyzed crosslinking reactions could potentially be exploited to prepare coatings that cure after only brief UV exposure, including epoxy-thiol and Michael addition.¹⁰ A major advantage of an epoxy-thiol system is that it does not contain any free isocyanates, which can pose potential health and safety issues.

In order to more fully understand the relationship between clearcoat formulations and curing kinetics, the curing rates of different model epoxy-thiol formulations were evaluated. These formulations were examined using FTIR spectroscopy, Raman spectroscopy, UV spectroscopy, and Vickers micro-hardness testing. The effect of additive concentrations and curing conditions has been elucidated.

Experimental

Materials

A model epoxy-thiol clearcoat was formulated for this study. The generic crosslinking mechanism for this system is shown in Fig. 2. The formulation consisted of bisphenol-A based epoxy resin (D.E.R. 330) and a thiol resin (trimethylolpropane tris-(3 mercaptopropionate)),

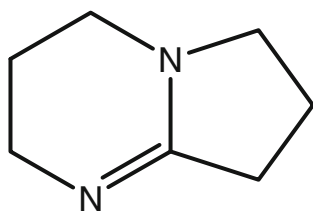


Fig. 1: Chemical structure of biazabicyclo-nonene (DBN)

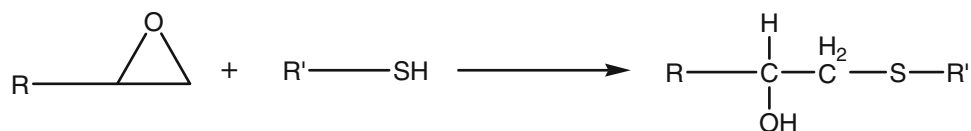


Fig. 2: Generic epoxy-thiol crosslinking reaction

each obtained from Sigma Aldrich (St. Louis, MO, USA). The final model clearcoat resin was mixed at a 1:1.357 ratio by weight of thiol to epoxy resin. This ratio was used in an effort to stoichiometrically balance the amount of thiol and epoxy functional groups.

Three additives were used to facilitate the UV curing of the epoxy-thiol clearcoat. The first additive, PL-DBN (Ciba, Inc., Basel, Switzerland), is a photolatent DBN species. The generic chemical structure of the PL-DBN is shown in Fig. 3. Two photosensitizers were used, benzophenone (BP) and Darocur ITX, with their structures shown in Fig. 3. ITX is a red shifted photosensitizer with a peak absorbance of ~380 nm. Benzophenone has a peak absorbance at ~340 nm. Both photosensitizers were obtained from Ciba Specialty Chemical, Inc. Additives were dissolved in acetone prior to mixing with the model resin system. The pKa of the PL-DBN increases upon exposure to UV light in the presence of the photosensitizers, initiating the base catalyzed crosslinking reaction. The pKa increase is thought to be due mainly to the photoinduced introduction of the amidine C=N double bond besides additional relief of steric hindrance upon cleavage of the PL-DBN.⁷

Sample preparation and curing conditions

Samples for IR spectroscopy were applied to silicon discs manually such that the –CH absorbance peak (at 2969 cm⁻¹) was between 1.1 and 1.2. Samples were transferred to a curing station and irradiated with an H&S Autoshot (Georgetown, ON) UVA400 lamp (clear filter) at a curing distance of 38 cm. A spectral power distribution (SPD) of the curing lamp is shown in Fig. 4, along with the absorbance spectra of the PL-DBN, BP, and ITX to illustrate the regions of the additives absorbencies that overlap the lamp's SPD. A small muffin fan was used to cool the sample and limit any heating by the UV lamp (samples reached ~26.5°C). After the irradiation period, the IR spectra were recorded periodically as curing proceeded. The UV curing intensity was ~183 W/m² between 320 and 390 nm.

Clearcoat samples for Raman spectroscopy were applied to cleaned, bare EG6060 steel panels with a draw down bar. Clearcoat samples were left affixed to the substrate during analysis. Clearcoat thicknesses ranged from 12 to 60 µm. Samples were again cured using the UVA400 lamp (with fan) at a curing distance of 38 cm.

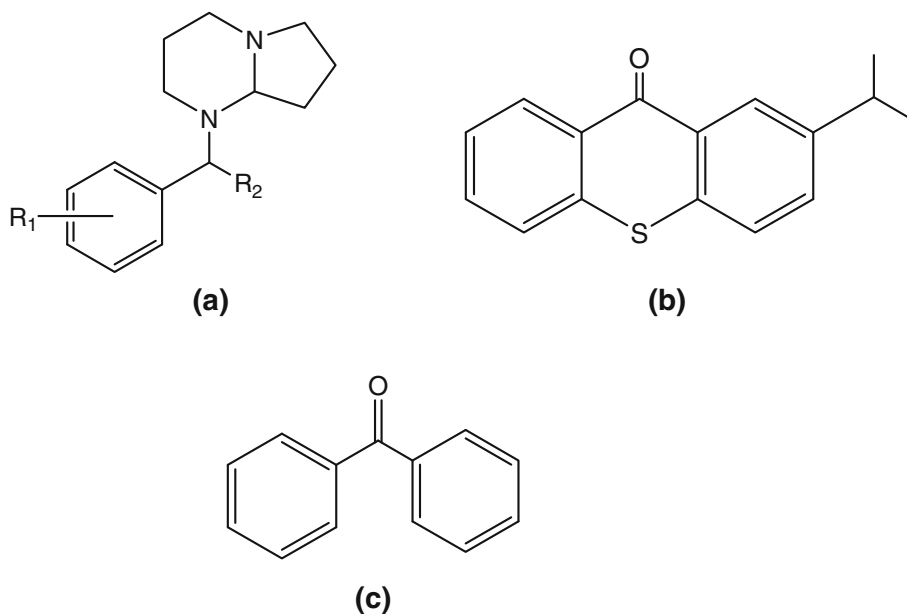


Fig. 3: Chemical structures of (a) generic photolatent DBN (PL-DBN), (b) Darocur ITX, and (c) benzophenone (BP)

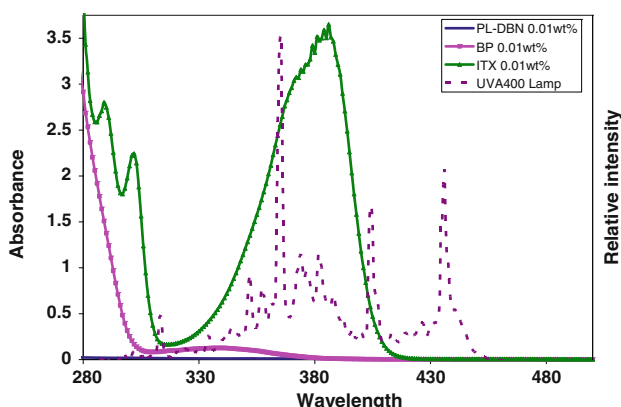


Fig. 4: Absorbance spectra of 0.01 wt% PL-DBN, BP, and ITX (in methylene chloride) overlaid on a spectral power distribution of the UVA400 curing lamp (relative intensity)

Clearcoat samples for Vickers micro-hardness were applied to cleaned, primed steel panels with a draw down bar. Clearcoat thicknesses ranged from 20 to 40 μm . Irradiation was conducted with and without the use of the small cooling fan to determine the impact of lamp heating on the final cure state of the clearcoat. Three irradiation times were used: 1.5, 5, and 10 min.

Cure monitoring

Transmission FTIR spectra were recorded with a BioRad FTS 175 IR microscope set to transmission mode. Samples were placed horizontally on the microscope stage in order to reduce any flow of the wet

clearcoat. A “wet”/time zero spectrum was taken of each sample prior to UV irradiation. After irradiation, absorbance spectra were taken after set time intervals to monitor cure as a function of time. Peak heights from these spectra were then used to quantify the concentration of thiol in the sample. Thiol concentration is inversely proportional to the cure state of the sample, from which the percent cure (P) of the sample could be calculated. The thiol peak located at 2569 cm^{-1} was ratioed to a reference peak (2969 cm^{-1}) and used to quantify the percent cure of the clearcoat sample at each time interval and create a plot of percent cure vs time after the start of irradiation (cure profile).

Raman spectra of clearcoats cured on steel panels were taken using a Renshaw 1000 Raman microscope that utilized a 633 nm HeNe laser and a $50\times$ objective. This instrument uses a holographic notch filter as a beam splitter to couple the laser light into the microscope and onto the sample and to reject laser light from the backscattered signal that goes to the spectrometer while passing the Raman-shifted spectrum. A second notch filter further reduces the backscattered laser intensity. Spectra could be recorded in either a static mode with a fixed spectra range of 900 cm^{-1} or in an extended mode in which the grating is stepped synchronously with the shifting of the charge in the charge-coupled device (CCD) array detector, in order to produce long, continuous scans.

Raman spectra were taken of the surface of the clearcoat and confocally (focusing through the clearcoat) of the bottoms of the clearcoats. Spectra were recorded using a static scan mode with an exposure time of 150 s and the grating centered in the polymer fingerprint region at 2850 cm^{-1} . Laser power on the sample was controlled at 3 mW and focused to a spot

size of 1–2 μm . Depth resolution was approximately 2–3 μm and spectra resolution about 6 cm^{-1} .

Raman spectra were taken of either the top or the bottom of a sample clearcoat over a given time period. The time needed to acquire a spectrum limited the monitoring to one surface per sample. A duplicate sample was run under the same curing conditions to measure the cure profile of the other clearcoat surface. As with the FTIR measurements, the thiol peak height was again measured in the Raman spectra. A second derivative transform was applied to the spectrum, after which the thiol peak (2572 cm^{-1}) was ratioed to a constant reference peak (2873 cm^{-1}). The second derivative was used to minimize the effect of fluorescence and baseline slope.¹¹ This ratio was used to calculate the percent cure of the top and bottom of each clearcoat sample after set time intervals and to create a cure profile for each sample surface.

UV spectroscopy

Transmission UV spectrum were collected using a Carl Zeiss, Inc., AxiotronTM MPM 800 microscope/spectrometer system with programmable stage. The spectra were taken through a clearcoat film that was drawn down onto a quartz plate. The spectra were collected from 250 to 500 nm.

Hardness testing

Vickers micro-hardness measurements were made with a Leco MHT Series 200 microhardness tester utilizing a 25 gmf load and a 10-s hold time. The indentation was measured though the instrument software using the 50 \times objective. The instrument software then calculated the HV hardness value for each sample.

Experimental design

A Taguchi Design of Experiments (DOE)^{12,13} was created to examine the main effects that impacted the rate of cure of the epoxy thiol system. Factors examined in this study were PL-DBN wt%, ITX wt%, BP wt%, and irradiation time. The DOE sample formulations are shown in Table 1. Cure profiles, from which second-order plots and rate constants were produced, were created from the FTIR data for each sample listed in the DOE.

Results

FTIR DOE

Cure profiles (percent cure vs time) of DOE samples #1–9 were created using the previously detailed FTIR

Table 1: Sample formulations used for the Taguchi DOE to monitor cure rate using FTIR

Sample	PL-DBN wt%	ITX wt%	BP wt%	Irradiation time (s)
1	2.50	0	0	30
2	2.50	1	1	60
3	2.50	2	2	90
4	3.25	0	1	90
5	3.25	1	2	30
6	3.25	2	0	60
7	4.00	0	2	60
8	4.00	1	0	90
9	4.00	2	1	30

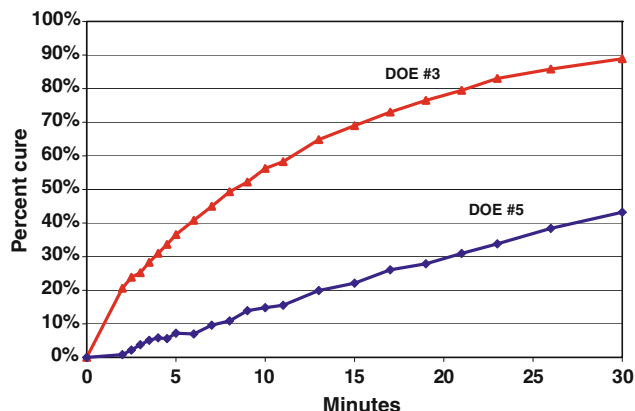


Fig. 5: Two example cure profiles (samples #3 and #5) as measured using the described FTIR method

method. Two replicates were run of each sample, resulting in a total of three cure profiles for each DOE sample. Two example profiles are shown in Fig. 5 for DOE samples #3 and #5. In order to quantify the rate constant for each of the samples, a second-order plot ($1/(1 - P)$ vs time) was made for the first 15 min of curing (Fig. 6). For this type of clearcoat curing, the initial cure rate, or time to tack free, is critical. The slope of the second-order plot was calculated for each sample and used to calculate the rate constant. The rate constant was calculated using the following equation¹⁴:

$$k_c = \text{Slope}/[-\text{SH}]_0 \quad (1)$$

where $[-\text{SH}]$ is expressed as equiv/kg. $[-\text{SH}]_0$ for this formulation was determined to be ~ 3.19 equiv/kg.

The calculated rate constants for each of the sample runs, along with the mean rate constant, are shown in Table 2. Sample #8 had the largest rate constant of all the samples.

Main effects plots were created to determine which factors had the most significant impact on cure rate (Fig. 7). The main effects plots show that irradiation

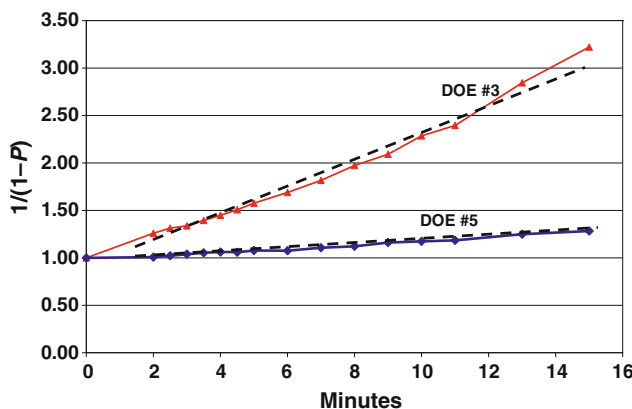


Fig. 6: Second-order plot of the cure profiles shown in Fig. 5 (samples #3 and #5)

Table 2: Rate constant for each DOE sample, along with the mean of the three runs

Rate constant (kg/equiv-min)

Sample	Run 1	Run 2	Run 3	Mean
1	0	0	0	0
2	1.16E-02	1.28E-02	1.47E-02	1.30E-02
3	4.50E-02	2.54E-02	2.71E-02	3.25E-02
4	5.89E-03	6.27E-03	6.08E-03	6.08E-03
5	6.21E-03	9.06E-03	5.86E-03	7.04E-03
6	1.66E-02	1.50E-02	1.20E-02	1.45E-02
7	9.62E-03	1.11E-02	1.27E-02	1.11E-02
8	3.57E-02	2.76E-02	3.48E-02	3.27E-02
9	1.07E-02	1.11E-02	9.44E-03	1.04E-02

time had the greatest impact on increasing the reaction rate constant. This is illustrated by the large, positive slope in the irradiation time main effect plot compared to the slopes of the three other factors. ITX wt% had a smaller, but still measurable, impact on cure rate (smaller, positive slope). BP wt% and PL-DBN wt% showed little change over the three levels, which indicated that it had no real impact on the cure rate of the system, within the ranges studied.

Raman/UV results

To examine how these FTIR curing profiles of thin (~8–10 µm) films translated to thicker, real-world clearcoat samples, Raman spectroscopy was used to create curing profiles of both the top and bottom of clearcoats with varying thicknesses. Sample #8 (4 wt% PL-DBN, 1 wt% ITX, 90-s irradiation) from the FTIR DOE was used for the Raman studies as it exhibited the highest cure rate of all nine DOE formulations. Two different “top” surfaces were measured along with four different “bottom” surfaces. The samples used for the “bottom” cure profiles had thicknesses of 12, 26, 33, and 60 µm, respectively (measured confocally). The cure profiles for these six surfaces are shown in Fig. 8. As the thickness of the clearcoat increased, the rate of cure at the bottom of the clearcoat decreased. The 12 µm thick sample had a bottom cure profile nearly identical to that of the top of the clearcoat. However, those measured that were thicker than 12 µm showed a clear reduction in cure rate, with the bottom of the 60 µm thick sample taking

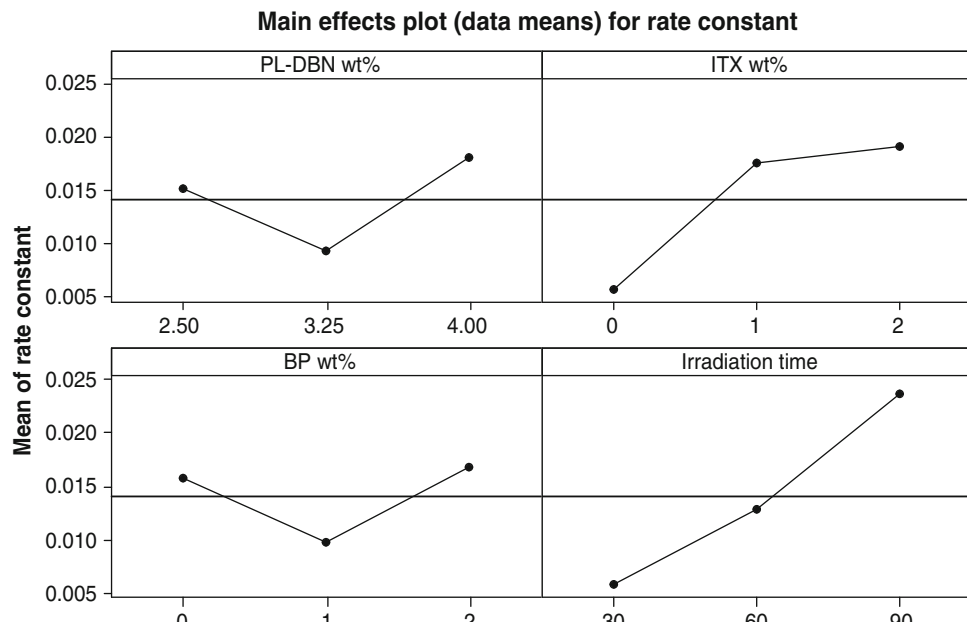


Fig. 7: Main effects plot created from Taguchi DOE results. Impacts of PL-DBN wt%, ITX wt%, BP wt%, and irradiation time are shown

nearly 30 min longer to reach ~70% cure than the bottom of the 12 µm thick sample.

To determine if the reduction in cure rate as a function of thickness was a result of the ITX reducing the amount of light that reached the depths of the clearcoat, an experiment was carried out where wet films of sample #8 were drawn down onto a piece of quartz and placed over (but not touching) a second wet film drawn down onto a steel panel. The cure profiles of the tops of the filtered clearcoats were measured using Raman spectroscopy. The results of this study are shown in Fig. 9. The cure rates of the two top surfaces of the filtered clearcoat films were clearly lower than the top of the control (standard curing) film. The top of the film that was filtered by a 70 µm thick film of clearcoat exhibited a similar cure profile to that of the bottom of the 60 µm control clearcoat. A similar

behavior was observed when comparing the top of the film filtered with a 42 µm thick clearcoat and the bottom of the 33 µm thick control film.

UV spectroscopy was used to quantify the absorbance/µm clearcoat thickness. These results were calculated by measuring a 41 µm thick wet film (sample #8) prior to curing (Fig. 10). It was determined that the formulation absorbed much of the UV radiation (~95.1% between 370 and 395 nm) and prevented the bottom of the clearcoat from receiving enough light to cure at a similar speed to the surface. The absorbance/µm clearcoat for sample #8 was ~0.032 between 370 and 395 nm.

Hardness results

Hardness testing was performed on samples made using sample #8 from the FTIR DOE to determine if irradiation time and temperature impacted the final

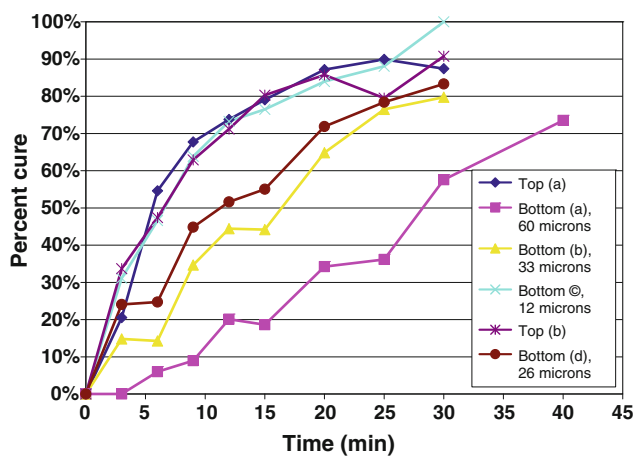


Fig. 8: Raman cure profiles for six different top and bottom “surfaces”. All surface measurements were taken from unique samples. All films were sample #8 formulations

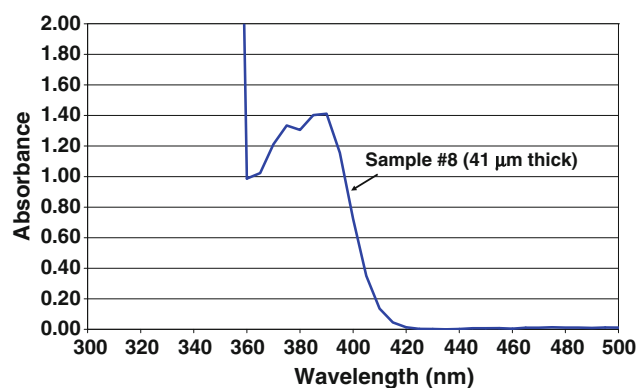


Fig. 10: UV absorbance spectra of drawn down film of sample #8 with a thickness of 41 µm

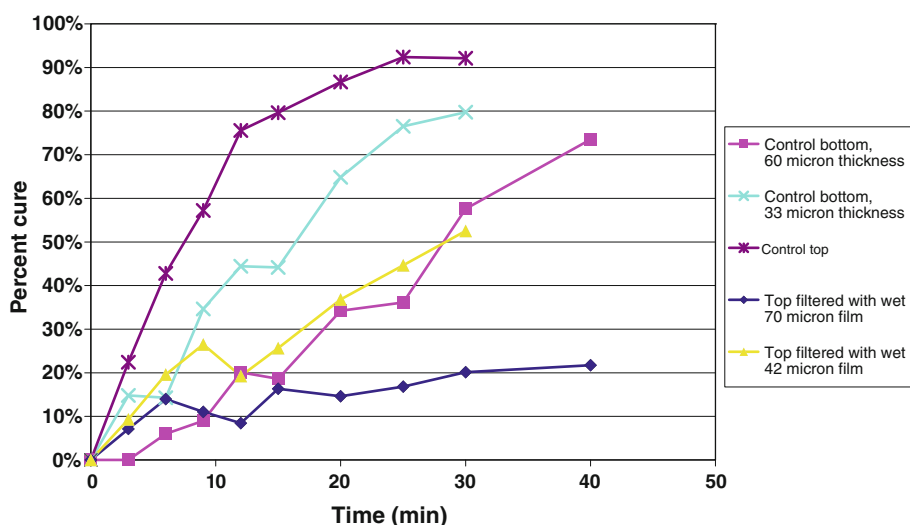


Fig. 9: Raman cure profiles for standard films (“control”), and samples filtered with a film drawn down on a quartz plate. All films were sample #8 formulations

Table 3: Vickers micro-hardness results for samples prepared using the sample #8 formulation from the FTIR DOE (results listed are averages of two measurements)

Irradiation time	UVA400 (33–35°C)	UVA400 (36–42°C)
Initial hardness results (HV@25 g)		
1.5 min	5	6
5 min	5	5
10 min	5	6
24-h hardness results (HV@25 g)		
1.5 min	7	7
5 min	7	5
10 min	7	7

physical properties of this epoxy-thiol clearcoat system. Samples without fan cooling reached a temperature of ~36–42°C during irradiation while samples cooled with a small muffin fan reached a temperature of ~33–35°C. Hardness results are shown in Table 3.

Initial hardness measurements were taken within a few hours after irradiation while the second set of measurements was taken 24 h later. Irradiation time did not impact the hardness of the final clearcoat, at either high or low temperature. After 24 h, the hardness of both sets of clearcoats increased slightly. A standard acrylic melamine OEM topcoat system was measured as a reference. This clearcoat had a micro-hardness of 8 HV@25 g.

Discussion

The DOE results indicated that the two factors of most importance to clearcoat cure rate were ITX wt% and irradiation time. BP wt% was shown to have limited impact on the curing rate of the clearcoat used in this study. The impact of PL-DBN on the cure rate did not change significantly across the tested loading levels. This does not necessarily indicate that BP is a poor photosensitizer, or that its interaction with PL-DBN does not result in an increase in pKa. The ineffectiveness of the BP is likely due to the light source chosen for this study, and the larger absorbance/SPD overlap seen for the ITX photosensitizer compared to the BP. It is possible that this same clearcoat system, utilizing a light source with a SPD, focused on the shorter UVA wavelengths, and even the UVB wavelengths would find that the BP wt% had a greater impact on the clearcoat cure rate. Maximum efficiency is achieved when the photosensitizers overlap the SPD of light source as much as possible. Additional formulation/process optimization is needed to increase the cure rates for these materials if they are to be applied and cured at standard application thicknesses (~50 µm). Clearcoats without PL-DBN do not cure at all, so the effectiveness is above some threshold.

The Raman studies showed that there was a dramatic gradient in the cure rates between the top

and bottom of clearcoats with thicknesses greater than 20 µm. Automotive clearcoat's thickness range from 40 to 50 µm, indicating that a gradient would exist if formulations similar to those studied here were applied to vehicles at standard film thicknesses. One solution to this problem would be to incorporate a photosensitizer that does not absorb broadly across the UV-A region. BP could perhaps be an alternative photosensitizer, but only in conjunction with a radiation source that possessed a peak overlapping with BP's absorbance (as was shown in the main effects analysis). Another option would be to simply reduce the amount of ITX used during formulation to reduce the absorbance per µm of the clearcoat. The main effects analysis showed that increasing the amount of ITX from 1 to 2 wt% did not improve the cure rate of the system. Reducing the ITX level to less than 1 wt% would likely improve the thru-cure and not significantly retard the overall curing rate. A more detailed formulation analysis would need to be run in order to optimize the quantity of ITX for this epoxy-thiol formulation.

Hardness measurements indicated no differences in clearcoat hardness across irradiation times. Hardness did increase slightly after the 24-h post-cure, but IR spectroscopy indicated that no additional crosslinking occurred after the initial curing and short post-cure.

While physical properties showed little variation as a function of formulations and irradiation times, other properties such as appearance and durability remain to be investigated, as these properties are strongly dependent upon the full paint system formulation and processing. The ability to use these formulations in pigmented systems is an open question at this time and will depend on the opacity of the pigments chosen and the mobility of the photolatent base in the binder system.

Conclusion

Isocyanate free, 2K epoxy-thiol clearcoat systems have been formulated, which cure rapidly upon exposure to UV light and slowly in the absence of UV exposure. Using experimental design methods, PL-DBN wt%, ITX wt%, and irradiation time/dose were shown to be crucial factors in the design of the clearcoat and curing system. Vickers micro-hardness analysis showed that while irradiation time had no impact on the final physical properties of the clearcoat, a 24-h ambient post-cure period increased the hardness of the final clearcoat. This system analysis and optimization is unique for the radiation source and clearcoat formulation used in this study. The results reinforce the need to spectrum match the photoactive species with the UV radiation source.

Acknowledgments The authors thank Eugene Sitzmann and Kurt Dietlicher for providing select raw materials needed for this study while also providing

technical consultation. The authors would like to thank Cindy Peters for her assistance in collecting the UV transmission spectra of the clearcoat films used in this study.

References

1. Zhang, H, Cattaneo, M, Li Bassi, G, “Zero VOC Coatings Cured by Sunlight.” *J. Coat. Technol.*, **72** (903) 77–79 (2000)
2. Jung, T, Valet, A, “Scratch Resistance and Weatherfastness of UV-curable Clearcoats.” *Macromol. Symp.*, **187** 531–542 (2002)
3. Koleske, JV, *Radiation Curing of Coatings*. ASTM International, West Conshohocken, PA (2002)
4. Evans, DC, Lancaster, JK, “The Wear of Polymers.” *Treat. Mater. Sci. Tech.*, **13** 85–139 (1979)
5. Hoyle, CE, Kinstle, JF, *Radiation Curing of Polymeric Materials*. American Chemical Society, Washington, DC (1990)
6. Riegel, ER, Kent, JA, *Riegel's Handbook of Industrial Chemistry*. Springer, New York (2003)
7. Dietliker, K, Huesler, R, Birbaum, J-L, Ilg, S, Villeneuve, S, Studer, K, Jung, T, Benkhoff, J, Kura, H, Matsumoto, A, Oka, H, “Advancements in Photoinitiators—Opening up New Applications for Radiation Curing.” *Prog. Org. Coat.*, **58** (2–3) 146–157 (2007)
8. Studer, K., et al., *Photolatent Bases: New Catalysts for UV-Curing of Coatings*, Radtech e!5: UV & EB Technology Conference 2006 Proceedings
9. Dogan, N, Klinkenberg, H, Reinerie, L, Ruigrok, D, Wijnands, P, Dietliker, K, Misteli, K, Jung, T, Studer, K, Contich, P, Benkhoff, J, Sitzmann, E, “Fast UV-A Curable Clearcoat.” *RadTech Report*, **20** (2) 43–52 (2006)
10. Noomen, A, “Application of Michael Addition Chemistry in Coatings Chemistry.” *Prog. Org. Coat.*, **32** 137–142 (1997)
11. Nichols, ME, Seubert, CM, Weber, WH, Gerlock, JL, “A Simple Raman Technique to Measure the Degree of Cure in UV-Curable Coatings.” *Prog. Org. Coat.*, **43** 226–232 (2001)
12. Roy, RK, *Design of Experiments Using the Taguchi Approach: 16 Steps to Product and Process Improvement*. Wiley, New York (2001)
13. Peace, GS, *Taguchi Methods a Hands-on Approach*. Addison-Wesley, Reading, MA (1993)
14. Hiemenz, PC, *Polymer Chemistry*, pp. 282–292. Marcel Dekker, Inc., New York, NY (1984)